

See discussions, stats, and author profiles for this publication at: <https://www.researchgate.net/publication/349453915>

# New Data on the headshield of *Parayunnanolepis xitunensis* (Placodermi, Antiarcha), with comments on nasal capsules in antiarchs

Article in *Journal of Vertebrate Paleontology* · February 2021

DOI: 10.1080/02724634.2020.1855189

CITATIONS

0

READS

154

2 authors:



Yajing Wang

Nanjing University

10 PUBLICATIONS 5 CITATIONS

[SEE PROFILE](#)



Min Zhu

Institute of Vertebrate Paleontology and Paleoanthropology, CAS, Beijing, China

233 PUBLICATIONS 4,335 CITATIONS

[SEE PROFILE](#)

Some of the authors of this publication are also working on these related projects:



redescription of *phymolepis cuifengshanensis* [View project](#)



Early Evolution of Sarcopterygii [View project](#)






## New data on the headshield of *Parayunnanolepis xitunensis* (Placodermi, Antiarcha), with comments on nasal capsules in antiarchs

Yajing Wang & Min Zhu


To cite this article: Yajing Wang & Min Zhu (2021): New data on the headshield of *Parayunnanolepis xitunensis* (Placodermi, Antiarcha), with comments on nasal capsules in antiarchs, *Journal of Vertebrate Paleontology*, DOI: [10.1080/02724634.2020.1855189](https://doi.org/10.1080/02724634.2020.1855189)

To link to this article: <https://doi.org/10.1080/02724634.2020.1855189>

 View supplementary material 



 Published online: 19 Feb 2021.

 Submit your article to this journal 

 View related articles 

 View Crossmark data 

## NEW DATA ON THE HEADSHIELD OF *PARAYUNNANOLEPIS XITUNENSIS* (PLACODERMI, ANTIARCHA), WITH COMMENTS ON NASAL CAPSULES IN ANTIARCHS

YAJING WANG <sup>1</sup> and MIN ZHU <sup>\*1,2,3</sup>

<sup>1</sup>School of Earth Sciences and Engineering, Nanjing University, Nanjing 210023, China, dg1929015@smail.nju.edu.cn;

<sup>2</sup>Key Laboratory of Vertebrate Evolution and Human Origins of Chinese Academy of Sciences, Institute of Vertebrate Paleontology and Paleoanthropology, Chinese Academy of Sciences, Beijing 100044, China, zhumin@ivpp.ac.cn;

<sup>3</sup>CAS Center for Excellence in Life and Paleoenvironment, Beijing 100044, China

**ABSTRACT**—The diversity in positions of nasal capsules has been well documented in various subgroups of placoderms or jawed stem gnathostomes. However, the condition in primitive antiarchs (i.e., the Yunnanolepidoidei) remains unclear, and the positional shift of nasal capsules in the Antiarcha has never been mentioned. Here we re-describe the headshield of *Parayunnanolepis xitunensis*, a yunnanolepidoid antiarch from the Lower Devonian of China, using X-ray computed tomography scanning. The study provides new anatomical details of the headshield including the sclerotic capsules, the visceral side of the rostral and pineal plates, and the dorsal profile of the endocranium. *Parayunnanolepis xitunensis* bears a pair of nasal capsules underlying the rostral plate between the eyes, resembling *Romundina* but differing from most euantriarchs, whose nasal capsules are encased in the preorbital recess in front of the eyes. A phylogenetic analysis based on a modified matrix indicates a stepwise forward migration of nasal capsules within antiarchs, accompanied by the innovation of the preorbital recess and the loss of the preorbital depression.

**SUPPLEMENTAL DATA**—Supplemental materials are available for this article for free at [www.tandfonline.com/UJVP](http://www.tandfonline.com/UJVP)

Citation for this article: Wang, Y. and M. Zhu. 2021. New data on the headshield of *Parayunnanolepis xitunensis* (Placodermi, Antiarcha), with comments on nasal capsules in antiarchs. *Journal of Vertebrate Paleontology*. DOI: 10.1080/02724634.2020.1855189.

### INTRODUCTION

The nasal capsule position is associated with the development of the anterior portion of the endocranium and the brain morphology; thus, it is an important trait for phylogenetic inference of early vertebrates (Goujet, 1984a; Dupret et al., 2017). Antiarchs, *Brindabellaspis* and acanthothoracids such as *Romundina*, and *Radotina* are grouped as ‘posterior-nosed’ placoderms (Dupret et al., 2014) by sharing an upper lip far anterior to the nasal capsules as in jawless fishes (at least including lampreys, osteostracans, and galeaspids). These forms have been consistently placed basal to other placoderms that bear terminal nasal capsules (Giles et al., 2015; Qiao et al., 2016; Zhu et al., 2016), such as arthrodiroids (Ørvig, 1975; Goujet, 1984b) and maxillate placoderms (Zhu et al., 2013, 2016, 2019).

The ‘posterior-nosed’ placoderms differ slightly in nasal openings and the spatial relationship of nasal capsules (King et al., 2018). These variable conditions raise difficulty in assessing the early evolutionary trajectory of nasal capsules at the origin of jawed vertebrates. In addition, unlike in *Brindabellaspis* (Young, 1980; King et al., 2018), *Romundina* (Ørvig, 1975; Dupret et al., 2017; King et al., 2018) and *Radotina* (Vaškaninová and Ahlberg, 2017), the homology of putative nasal structures in primitive antiarchs is controversial.

There are three interpretations of the position of nasal capsules and nares in yunnanolepidoids. Zhang (1978) mentioned the similarity between the nares of *Yunnanolepis* and *Remigolepis* and

proposed the potential relationship between the nasal capsules and the preorbital depression. Young (1984) further inferred that the nasal capsules of yunnanolepidoids were restricted to a narrow region of the preorbital depression and considered that their nares should open laterally into the lateral extensions of the preorbital depression. Nevertheless, this viewpoint is inconsistent with the fact that the floor of the preorbital depression is evenly ornamented with prominent tubercles (Janvier and Pan, 1982; Long and Werdelin, 1986; Zhu, 1996; Zhu and Janvier, 1996). Zhang (1980) provided the second interpretation that the nasal capsules with lateral nares extend beneath the premedian plate on both sides of the subpremedian ridge, based on a rostral plate preserved in situ. Long and Werdelin (1986) offered the third interpretation that the nasal capsules in yunnanolepidoids are situated beneath the rostral plate by comparison to the state in *Romundina*. In summary, yunnanolepidoids were generally thought to have lateral nasal openings, but the position of the nasal capsules is yet to be settled.

Since the first description by Zhang et al. (2001), *Parayunnanolepis xitunensis* has been widely involved in phylogenetic analyses of early gnathostomes (Zhu et al., 2013, 2016, 2019; Dupret et al., 2014; Brazeau and Friedman, 2015; Giles et al., 2015; Long et al., 2015) as an early representative of primitive antiarchs. To complement the character set of *P. xitunensis*, here we re-describe its headshield through high-resolution X-ray computed tomography (CT) scanning and make some comments on the evolution of nasal capsules in antiarchs.

**Institutional Abbreviation**—**IVPP**, Institute of Vertebrate Paleontology and Paleoanthropology, Chinese Academy of Sciences, Beijing, China.

**Anatomical Abbreviations**—**ADL**, anterior dorsolateral plate; **aln**, anterior lamina of the rostral plate; **AMD**, anterior median

\*Corresponding author.

Color versions of one or more of the figures in the article can be found online at [www.tandfonline.com/ujvp](http://www.tandfonline.com/ujvp).

dorsal plate; **amp**, anterior median process of the sclerotic ring; **apr**, anterior preorbital ridge; **ap.R**, anterolateral process of the rostral plate; **AVL**, anterior ventrolateral plate; **a.pq**, attachment for the levator quadrate muscular; **a.spr**, attachment area for sub-premedian ridge; **a1**, **2**, anterior and posterior processes on the submarginal plate; **bu.S3**, bulge on the inner side of the third sclerotic plate; **cf.PrM**, contact face for premedian plate; **cr.pm**, paramarginal crista; **cr.po**, postorbital crista; **c.acs**, **c.pcs**, anterior and posterior cavities for craniospinal processes; **c.P**, cavity for pineal organ; **dc**, dorsal corner of the suborbital plate; **dg.S2**, dorsal groove on the second sclerotic plate; **dln**, dorsal lamina of the rostral plate; **dl.S**, dorsal lamina of the submarginal plate; **dsc**, semicircular depression; **d.ap**, **d.pp**, depressions caused by anterior and posterior postorbital processes; **d.end**, opening for endolymphatic duct; **d.S2**, dorsal lamina of the second sclerotic plate; **eth.c**, ethmoid commissure; **eth.e**, ethmoid eminence; **eye**, eyeball; **eys**, eyestalk attachment area; **fm**, unpaired insertion fossa for levator muscles; **f.am**, adductor fossa; **f.pr.d**, floor of the preorbital depression; **f.S1**, **f.S3**, fragments of the first and third sclerotic plates; **ifc.a**, **ifc.p**, anterior and posterior branches of the infraorbital sensory canal; **ifc.ot**, otic division of the infraorbital sensory canal; **g**, pit on the post-pineal plate; **g.S1**, **g.S3**, grooves for eyestalk attachment on the first and third sclerotic plates; **iln**, internasal lamina of the rostral plate; **La**, lateral plate; **lc**, main lateral line canal; **mpl**, middle pitline groove; **mr**, medial ridge on the postpineal plate; **na**, nasal sac; **nm**, obducted nuchal area; **Nu**, nuchal plate; **o.PP**, area overlapped by postpineal plate; **P**, pineal plate; **Pi**, pineal opening; **pl.P**, posterolateral process of the pineal plate; **PM**, postmarginal plate; **PNu**, paranuchal plate; **PP**, postpineal plate; **ppl**, posterior pitline groove; **ppr**, posterior preorbital ridge; **pp.th**, postpineal thickening; **PrM**, premedian plate; **proc**, preobstacnic corner of headshield; **pr.av**, anteroventral process of the suborbital plate; **pr.d**, preorbital depression; **pr.r**, preorbital recess; **p.S1**, posterior lamina of the first sclerotic plate; **R**, rostral plate; **rec.PP**, recess within postpineal plate; **RoPi**, rostro-pineal plate; **r.if**, infraorbital ridge bordering sensory canal; **r.md**, ridge marking course of mandibular branch of trigeminal nerve; **r.pq**, ridge supporting palatoquadrate; **r.spr**, subpremedian ridge; **r.S2**, ventral ridge on the second sclerotic plate; **r.v**, incurved ventral rim of the suborbital plate; **Scl1–3**, first, second and third sclerotic plates; **SM**, submarginal plate; **SL**, semilunar plate; **SO**, suborbital plate; **socc**, supraoccipital cross-commissural pitline groove; **sop**, supraoccipital pit; **spi**, spiracle; **v.S2**, ventral lamina of the submarginal plate; **v.S2**, ventral lamina of the second sclerotic plate.

## MATERIAL AND METHODS

### Material

The re-description here is based on the holotype of *P. xitunensis* (V11679.1), which was collected from the middle part of the Xitun Formation at Cuifengshan in Qujing city, Yunnan Province, China. It was prepared mechanically from muddy limestone with pneumatic air scribes and needles and is housed at the Institute of Vertebrate Paleontology and Paleoanthropology (IVPP).

The high-resolution CT scanning was carried out at the Key Laboratory of Vertebrate Evolution and Human Origins, Chinese Academy of Sciences on the CT scanner, which was developed by the Institute of High Energy Physics, Chinese Academy of Sciences (Wang et al., 2019). The X-ray tube was operated at 150 kV, 0.1 mA, 1000 ms exposure time, a 1-mm aluminum filter, 1440 projections, a rotation step 0.25° and 16.6 µm pixel size resolution. Raw files were pre-processed using VG Studio 2.1 and then imported into Mimics 19.0 to reconstruct the 3D models.

### Phylogeny

We ran a phylogenetic analysis using a revised version of the matrix compiled by Wang and Zhu (2018), with some character codings of *P. xitunensis* updated from the present study. We also added one additive character in the matrix (Character 80, the position of nasal sacs relative to eyes: at the same level with eyes [state 0], slightly in front of eyes [state 1], in front of eyes [state 2]). The modified data set comprises 44 taxa (including two out-group taxa *Kujdanowiaspis* and *Romundina*) and 80 characters. More details, including additional references and character coding modification, are provided in the Supplemental Data 1 and 2.

Data were coded in Mesquite 3.61 (Maddison and Maddison, 2019), and then exported as a TNT file. Parsimony analysis was performed in TNT v 1.5 (Goloboff and Catalano, 2016) using traditional search and TBR branch swapping. Branch support was estimated with the bootstrap values by 100 pseudoreplicates and Bremer decay indices. All characters were unordered (except Characters 19, 49, 50, and 80).

## SYSTEMATIC PALEONTOLOGY

Class PLACODERMI McCoy, 1848

Order ANTIARCHA Cope, 1885

Suborder YUNNANOLEPIDOIDEI Gross, 1965

Family YUNNANOLEPIDIDAE Miles, 1968

*PARAYUNNANOLEPIS XITUNENSIS* Zhang, Wang,  
and Wang, 2001  
(Figs. 1–3)

**Holotype**—IVPP V11679.1 (Zhang et al., 2001), an articulated head and trunk shield with the post-thoracic body covered by scales.

**Referred Material**—IVPP V11679.2, the left pectoral fin articulated against the partial trunkshield; IVPP V11679.3, the single left anterior dorsolateral plate; IVPP V9059.1–3, three articulated head and trunk shield specimens.

**Locality and Horizon**—Xitun Formation (late Lochkovian) of Cuifengshan, Qujing city, Yunnan Province, China.

**Emended Diagnosis**—A small-sized yunnanolepid antiarch distinguished by the following combination of characters: a large orbital fenestra at about one-third of the head length; the infraorbital sensory canal having two branches around the orbit; the semicircular preorbital depression having a roof; the presence of the supraoccipital cross-commissural pitline groove; the presence of the postpineal endocranial process; and the presence of the two craniospinal processes.

**Remarks**—The revised diagnosis here is focused on the head characters. It differs from the original diagnosis by Zhang et al. (2001), which is composed of general characters in yunnanolepids. Young and Zhang (1996) described three specimens (IVPP V9059.1–3) that were referred to *Phymolepis cuifengshanensis*, from the same site as the holotype of *P. xitunensis*. Recently, Wang and Zhu (2018) remarked that IVPP V9059.1–3 are distinguishable from *P. cuifengshanensis* in headshield features. According to our new examination, we re-assigned these specimens (IVPP V9059.1–3) to *P. xitunensis*.

## DESCRIPTION

### Headshield

The dorsal side of the headshield is characterized by a relatively large orbital fenestra at about one-third of the head length (Fig. 1B), a distinctive sensory canal pattern (see below), and a semicircular preorbital depression formed by a strongly concave posterior lamina of the premedian plate. The outline of the headshield reaches the maximum width at the



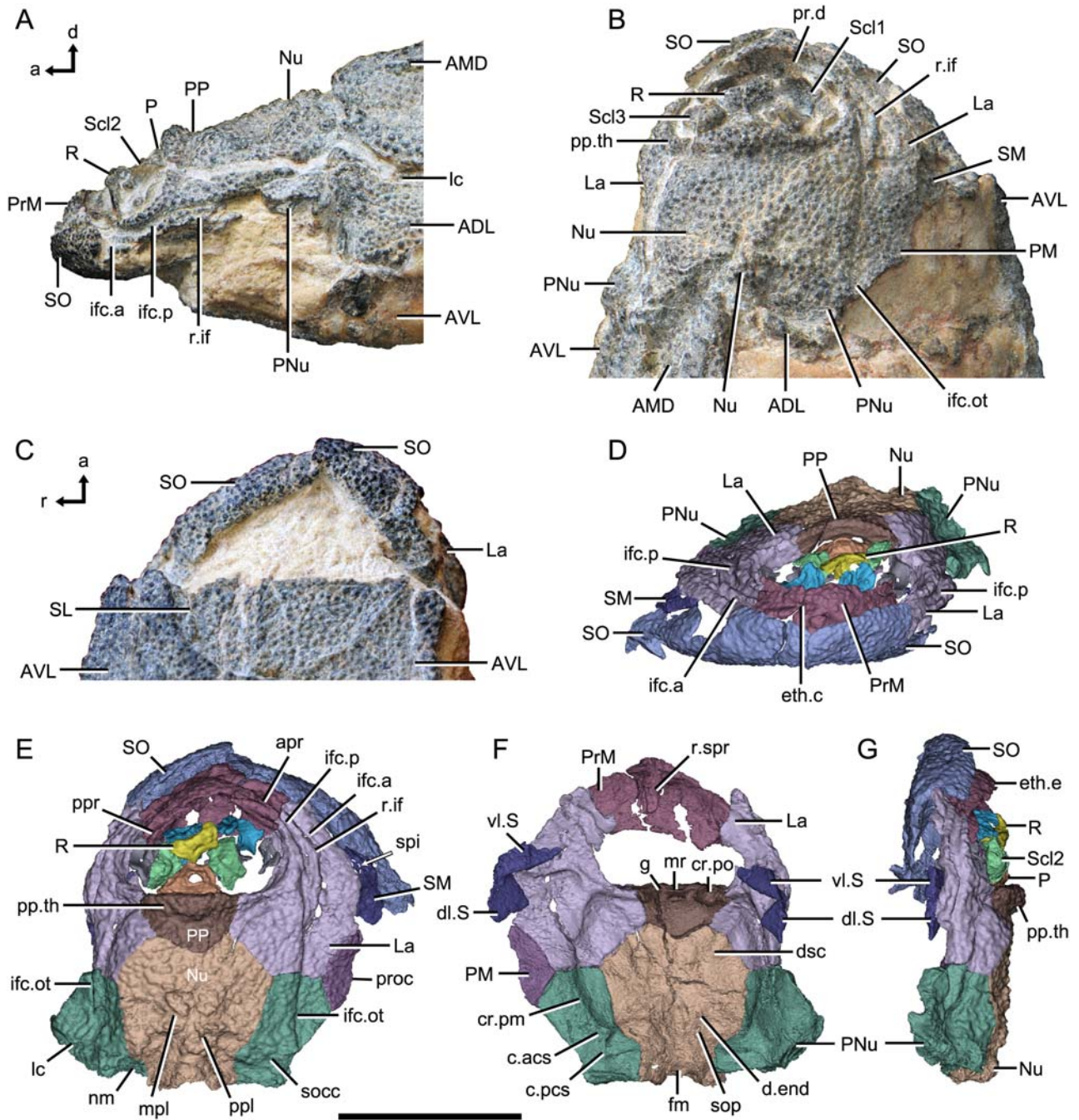


FIGURE 1. Headshield of *Parayunnanolepis xitunensis* (IVPP V11679.1). **A–C**, headshield with the articulated trunkshield in **A**, left lateral, **B**, dorsal, and **C**, ventral views. **D–G**, reconstruction of the headshield based on high-resolution CT scanning in **D**, anterior, **E**, dorsal, **F**, ventral, and **G**, left lateral views. The dashed line in **E** delineates the spiracle. Arrows indicate the orientation of the specimen: **a**, anterior direction; **d**, dorsal direction; **r**, right direction. For abbreviations, see text. Scale bar equals 5 mm.

level of the preobstantic corner. The postpineal thickening is most developed on the postpineal plate (Fig. 1E; Young and Zhang, 1996:fig. 4), and its maximum length occupies approximately half of the plate length. In visceral view, internal openings for endolymphatic ducts and supraoccipital pits (Figs. 1F, 2B) are located at the same longitudinal line and medial of the semicircular depression.

**Sclerotic Ring**—The sclerotic capsule of *P. xitunensis* consists of the first, second, and third sclerotic plates (Fig. 2D–H; Fig. S1 in Supplemental Data 1), with the same suture position as *Asterolepis* (Lukševičs, 2001a:fig. 6) and *Bothriolepis* (Stensiö, 1948:fig. 21c). The first sclerotic plate bears a robust anterior median process and an inner groove (Fig. 2G, I). The second sclerotic plate can be further divided into dorsal and ventral

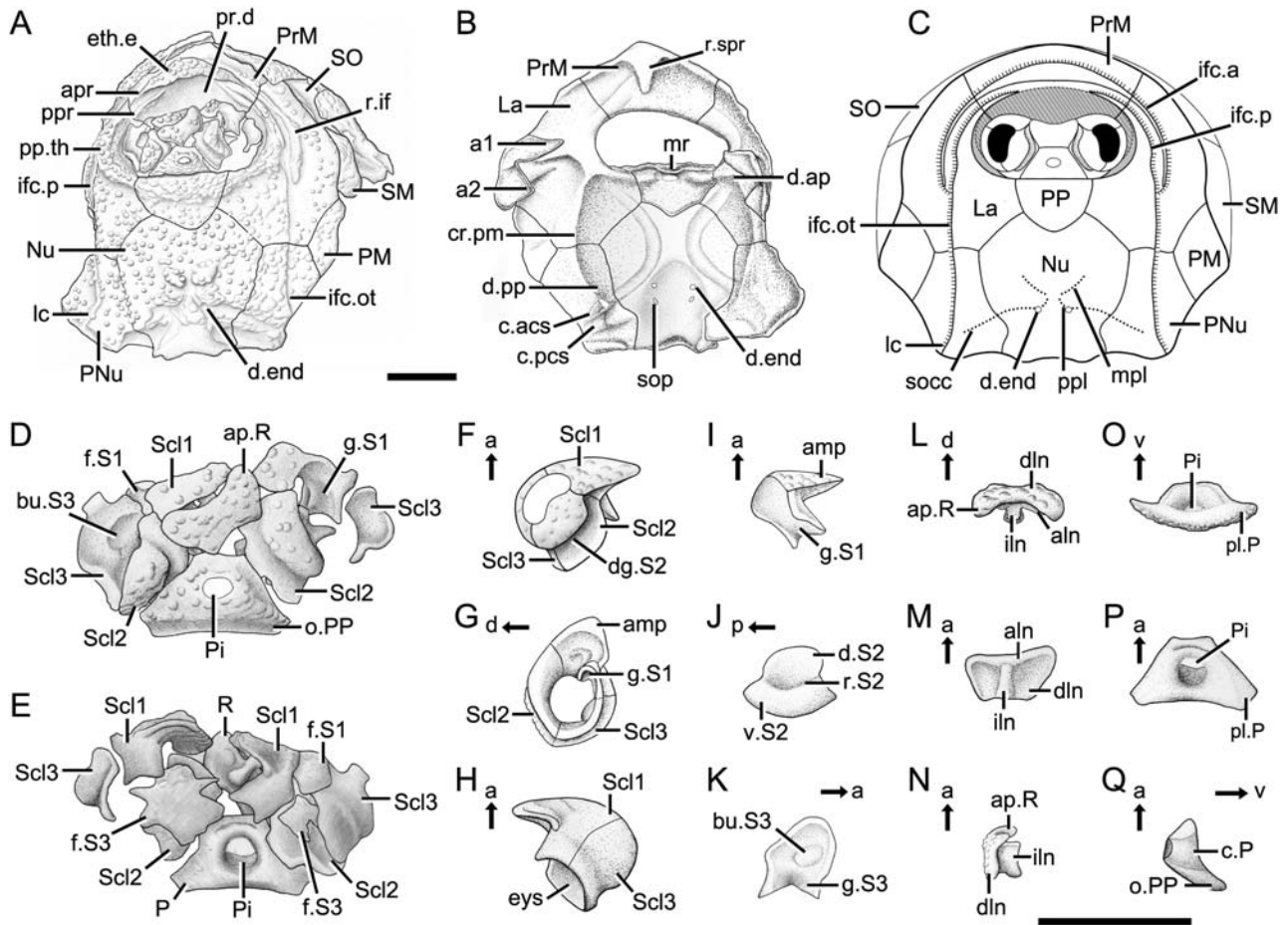


FIGURE 2. *Parayunnanolepis xitunensis* (IVPP V11679.1) based on high-resolution CT scanning. **A, B**, interpretative drawings of the headshield in **A**, dorsal, and **B**, ventral views. **C**, reconstruction (not to scale) of the headshield in dorsal view. **D, E**, orbito-nasal ossifications in **D**, dorsal, and **E**, ventral views. **F–H**, restored left scleritic ring in **F**, dorsal, **G**, posterior, and **H**, ventral views. **I–K**, scleritic plates; **I**, first, **J**, second, and **K**, third scleritic plates in ventral view. **L–N**, rostral plate in **L**, anterior, **M**, ventral, and **N**, right lateral views. **O–Q**, pineal plate in **O**, posterior, **P**, ventral, and **Q**, right lateral views. Arrows indicate the orientation of the specimens: **a**, anterior direction; **d**, dorsal direction; **p**, posterior direction; **v**, ventral direction. For abbreviations, see text. Scale bars equal 2 mm.

laminae by a deep dorsal groove on the outer surface or a developed ridge on the ventral surface (Fig. 2F, J). The convex dorsal lamina is ornamented with tubercles, which become finer outwards. The third sclerotic plate bears a bulge on the inner side near the lowermost part of the sclerotic ring (Fig. 2D, K).

As in other antiarchs (Stensiö, 1948; Lukševičs, 2001a), the sclerotic capsule in *P. xitunensis* lacks an ossified fundus that encloses the visceral side of the eyeball. Instead, there is a large-diameter tubular sclerotic passage with an everted posterior rim (Fig. 2H). This passage occupies the center position of the visceral side of the eyeball as does the eyestalk attachment area in other placoderms (Goujet and Young, 2004:fig. 5). It is reasonable to assume that this large-diameter passage in antiarchs carried, at least, optic nerve II and the major artery for the eyes.

**Pineal Plate**—This plate has developed posterolateral processes (Fig. 2O, P) as in euantiarchs. The narrow rostral and pineal plates in *P. xitunensis* reflect a small orbital spacing when compared with asterolepidoids, e.g., *Remigolepis* (Stensiö, 1948: fig. 16) and *Asterolepis* (Lukševičs, 2001a:fig. 7A). The pineal plate bears an unornamented rim (Fig. 2D), which is overlapped

by the postpineal plate. An external oval pineal foramen (Fig. 2D) is situated on the apex of the dorsal surface of the rostral plate, with radially arranged tubercles around. The pineal duct is enlarged internally and displays a rounded internal opening (Fig. 2E, Q) on the ventral side. The apparent size difference between the external and internal pineal openings is also present in *Bothriolepis* (Stensiö, 1948:fig. 23).

**Preorbital Depression and Premedian Plate**—A triangular eminence (Figs. 1G, 2A, 3B) rises from the premedian plate to form the roof for the preorbital depression. The eminence laterally extends to form the anterior preorbital ridges (Fig. 1E). Compared with other yunnanolepids (Zhang, 1978:fig. 1a; Zhang, 1980:fig. 1a), the preorbital depression in *P. xitunensis* differs in its semicircular profile (Figs. 1B, 2A) as in *Minicrania lirouyui* (Zhu and Janvier, 1996:fig. 4), and fine ornamentation. The floor of the preorbital depression (Fig. 3A), no more than a sloping surface sinking to the level of the suborbital fenestra, lacks prominent tubercles but undulates slightly in the mid-line region (Fig. S2B). Flat tubercles are sparsely distributed on the orbital wall just above the lateral portion of the preorbital depression (Fig. S2A).



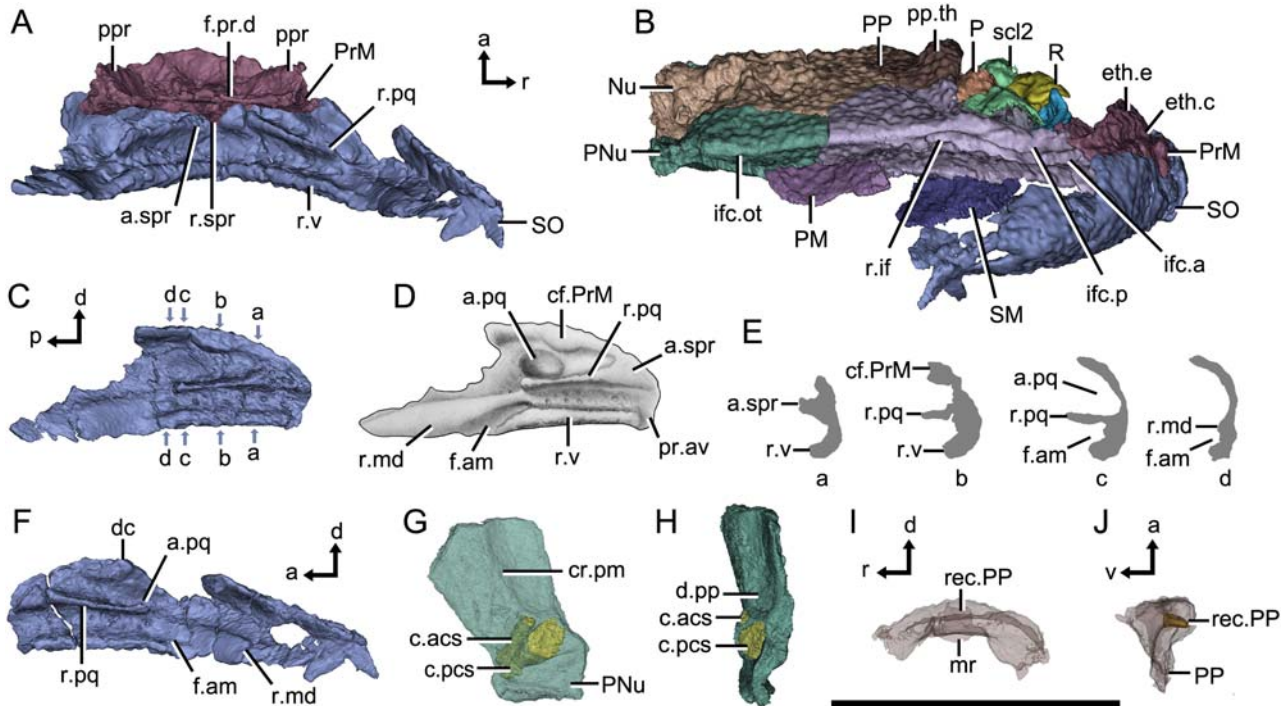


FIGURE 3. *Parayunnanolepis xitunensis* (IVPP V11679.1) based on high-resolution CT scanning. **A**, suborbital and premedian plates in posterior view. **B**, headshield in right lateral view. **C**, left suborbital plate in visceral view. **D**, interpretative drawing of **C**. **E**, axial sections at the levels indicated by blue arrows in **C**. **F**, right suborbital plate in visceral view. **G**, semi-transparent right paranuchal plate in ventral view. **H**, right paranuchal plate in mesial view. **I, J**, transparent postpineal plate showing the postpineal cavity in **I**, anterior, and **J**, left lateral views. Arrows indicate the orientation of the specimens: **a**, anterior direction; **d**, dorsal direction; **r**, right direction; **v**, ventral direction; **p**, posterior direction. For abbreviations, see text. Scale bar equals 5 mm.

On the visceral surface, a robust subpremedian ridge (Fig. 1F) develops from the rostral angle of the headshield to the two-thirds midline length of the premedian plate. This ridge also exists in *Mizia parvus* (Zhang, 1980:fig. 1c; Zhu, 1996) and *Yunnanolepis chii* (Wang and Zhu, 2018:fig. 12). It might be homologized with the premedian ridge in euantiarchs, such as *Bothriolepis* (Long and Werdelin, 1986:fig. 13D) and *Microbrachius* (Hemmings, 1978:fig. 26A).

**Submarginal Plate**—This is a slender plate lying between the headshield and the suborbital plate. The plate can be subdivided into ventral and dorsal laminae (Fig. 1F, G). A spiracular opening is formed by the notched mesial margin of the submarginal plate and the lateral margin of the lateral plate (Fig. 1E). The submarginal plate attaches to the headshield through its anteroventral and posteroventral processes (Fig. 2B). The strongly developed anteroventral process steps deep into the visceral surface of the headshield similar to that of *Qilinyu rostrata* (Zhu et al., 2016:fig. S3G). The posteroventral process covers the spiracular groove (Fig. S2C), as in *Bothriolepis karawaka* and *B. longi* (see Lukševičs, 2001b).

Young and Zhang (1996:fig. 5B) identified two dermal elements anteriorly to the ‘submarginal plate’ as potential prelateral and infraprelateral plates in *P. xitunensis*. Still, as seen in the holotype, no additional space is available for the presence of these two extra elements (Fig. 3B). The elongate submarginal plate lies above, and closely attaches to the suborbital plate in *P. xitunensis*. This arrangement is also seen in *Entelognathus* (Zhu et al., 2013:fig. S12b), *Qilinyu* (Zhu et al., 2016:fig. S1C), and arthrodires (Boyle and Ryan, 2017:fig. 2), but differs from that of euantiarchs. Furthermore, unlike that of euantiarchs, the submarginal plate of *P. xitunensis* is smaller than the suborbital plate. How these changes of the submarginal plate were associated with the jaw suspension is uncertain.

**Suborbital Plate**—This is proportionately more elongate ( $L/H = 4.1$ , see Fig. 1C) than that of euantiarchs, such as *Nawagiaspis* (Young, 1990:fig. 8) and *Pterichthyodes* (Hemmings, 1978:fig. 6). In visceral view, the concave surface displays a long ridge (Fig. 3A, C–F) for supporting the palatoquadrate as in other antiarchs, e.g., *Bothriolepis* (Young, 1984). The swollen anterior end of the ridge (Fig. 3A, D) contacts with the anterior portion of the subpremedian ridge. Another extensive contact area for the premedian plate (Fig. 3D–F) is around the dorsal corner of the plate. The convex anterior margins of the left and right suborbital plates indicate that they are separated, while a weakly developed anteroventral projection (Fig. 3D) might be a site for ligamentous or cartilaginous connection between them as inferred for *Bothriolepis* (Young, 1984). The ventral margin of the plate folds inward to form a narrow rim (Fig. 3A, D, E), which displays blunt tubercles in random order on the ventral surface.

At the posterior end of the ridge for palatoquadrate, two prominent fossae are located below and above it. The lower one (Fig. 3D–F) in open communication with the ventral space, corresponds to the adductor fossa in other placoderms (e.g., Young, 1979:figs. 13C, 14; Young, 1986:figs. 12, 13). The upper fossa (Fig. 3D–F) faces anteromedially and is the most concave area of the suborbital plate. The same fossa in *Bothriolepis* where the palatoquadrate was inferred to attach endocranium by an articular surface on the lingual surface, was assumed to be the dorsal extension of the adductor fossa (Young, 1984). Crucial evidence to support this interpretation was the connection between those two fossae, but this is not the case in *P. xitunensis*. By comparison to other placoderms (Miles, 1971:fig. 33; Goujet, 1984b:fig. 43c), the upper fossa more likely represents the attachment area for the levator palatoquadrate muscle. The two fossae are separated from each other by a robust thickening (Fig. 3D), which just follows the

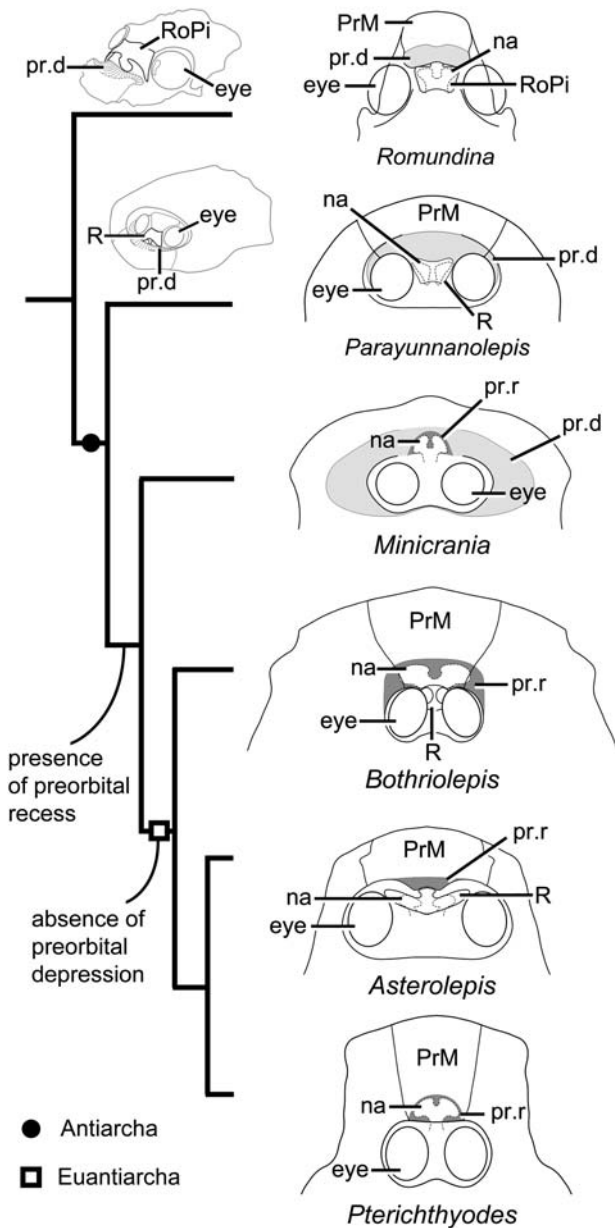


FIGURE 4. Transformations of nasal capsules in antiarchs and the out-group *Romundina*. The reconstruction of *Romundina* is based on Dupret et al. (2014, 2017); *Minicrania* is based on Zhu and Janvier (1996); *Asterolepis* is based on Obruchev (1933) and Lukševičs (2001a); *Bothriolepis* is based on Stensiö (1948) and Young (1984); *Pterichthyodes* is based on Hemmings (1978). Simple most parsimonious tree obtained from the phylogenetic analysis. For abbreviations, see text. Not to scale.

ridge for palatoquadrate. It is in accord with the thickening being assumed as the “posterior extension of the ridge supporting the palatoquadrate” in *Bothriolepis* (Young, 1984). It also occupies the same position as the “ridge marking course of mandibular branch of trigeminal nerve” around the metapterygoid in arthrodires (Miles, 1971:fig. 32c; Young, 1979:fig. 14).

### Nasal Structure

The rostral plate consists of the dorsal, anterior, and internasal laminae (Fig. 2L–N). Tubercles are only present on the dorsal

surface of the dorsal lamina. The anterior margin of the rostral plate is concave in the middle section as in *Yunnanolepis* (Zhang, 1978). Thus the external naris is positioned close to the midline of the rostral plate and bounded laterally by well-developed anterolateral processes (Fig. 2D) as in asterolepidoids (Stensiö, 1948:fig. 16; Lyarskaja, 1981:fig. 67), instead of at the lateral notch of the first sclerotic plate as previously reconstructed (Young and Zhang, 1996).

A thin anterior roof for the external nares (Fig. 2L) has been formed by the incurved dorsal lamina. The internasal lamina (Fig. 2L–N) develops under the dorsal lamina and does not exceed the anterior lamina anteriorly. As such, the nasal capsules inevitably lie beneath the rostral plate, and the paired external nares face anteriorly. Considering the proportion of the rostral plate, the nasal capsules in *P. xitunensis* are small, as previously suggested by Long and Werdelin (1986). The concave posterior margin of the rostral plate makes it difficult to speculate how it contacts against the straight anterior margin of the pineal plate (Fig. 2D).

The new data herein corroborate that *P. xitunensis* (and perhaps other yunnanolepidoids) resembles *Romundina* (Dupret et al., 2017:fig. 16) in nasal capsules lying beneath the rostral plate between the eyes, posterior to the preorbital depression of the premedian plate.

### Sensory Canal System

The short middle pitline, the posterior pitline and long supraoccipital cross-commissural pitline grooves (Fig. 2C) coexist on the nuchal plate, as shown by ornamentation on the surface. An infraorbital ridge (Fig. 2A) on the lateral plate is confluent with the anterior preorbital ridge on the premedian plate. This connection divides the infraorbital canal into anterior and posterior branches (Figs. 1A, E, 2C; Fig. S2F), which correspond to shallower ventral and deeper dorsal grooves described by Young and Zhang (1996), respectively. The anterior sensory branch runs along the infraorbital ridge and anterior preorbital ridge, and then passes across the midline of the premedian plate to be the ethmoidal commissure (Figs. 1D, 2C) without leaving off the headshield. This trajectory is thus slightly different from the previous reconstruction (Young and Zhang, 1996), and indicates that the anterior branch probably corresponds to the “principal section of infraorbital sensory line” of *Bothriolepis* (Young, 1988:fig. 42). The posterior branch bounded medially by the connection of the postpineal thickening and the posterior preorbital ridge (Fig. 1E), passes into the preorbital depression. The posterior branch is more likely to be a derived feature that *P. xitunensis* shares with *Minicrania lirouyui* (Zhu and Janvier, 1996:fig. 4) and *Yunnanolepis* sp. (Tōng-Dzuy and Janvier, 1990:fig. 12a1).

### Endocranium

The post-orbital portion of the braincase can be outlined by the otic-occipital depression of the headshield in *P. xitunensis*. Two craniospinal processes immediately behind the blunt posterior postorbital process, are accommodated into two cavities in sequence (Fig. 3G, H) as in *Minicrania lirouyui* (Zhu and Janvier, 1996:fig. 6b). The anterior cavity is slender with a small opening, and the posterior one is robust with a large opening.

Noteworthy is the presence of a process beneath the postpineal plate, as indicated by a recess (Fig. 3I, J). The postpineal recess lies at the same level as the anterior postorbital process, which houses the exit for a hyomandibular branch of the facial nerve in acanthothoracids (Dupret et al., 2017). Therefore, the recess in *P. xitunensis* seems topologically to correspond to the trigeminal recess on the endocranial dorsal side of *Romundina* (Dupret et al., 2017:figs. 4–6).



## DISCUSSION

## Phylogenetic Result

The phylogenetic analysis resulted in 726 most parsimonious trees with a tree length of 186 (Supplemental Data 3). The strict and majority-rule consensus trees are shown in Figure S3 in Supplemental Data 1. The results match with the previous study (Wang and Zhu, 2018), implying that the distribution of the new character (the position of nasal sacs relative to eyes) and the character combination of *P. xitunensis*, fit well with the former phylogenetic scenario of antiarchs. In our analysis, *Parayunnanolepis* was recovered in a polytomy with *Mizia* and *Phymolepis* by sharing an unambiguous feature: Character 30 (state 1), absence of the supraorbital canal. State 2 (nasal sacs in front of eyes) of character 80 supports the branch leading to advanced antiarchs (*Minicrania* + Sinolepididae + Euantriarcha), and State 1 (nasal sacs slightly in front of eyes) is shared by a clade grouping *Wurungulepis*, *Stegolepis*, *Pambuluspis*, *Asterolepis*, *Remigolepis*, and *Byssacanthus*, see Figure S4 in Supplemental Data 1.

## Nasal Capsule Transformation

For antiarchs bearing the preorbital recess like *Bothriolepis*, *Minicrania*, and *Pterichthyodes* (Fig. 4), the nasal capsules were generally thought to reside within this recess on the visceral side of the premedian plate (Stensiö, 1948; Hemmings, 1978; Young, 1984; Zhu and Janvier, 1996; Johanson et al., 2019). Exceptions are *Asterolepis* (Lukševičs, 2001a) and *Remigolepis* (Johanson, 1997), which have a reduced preorbital recess. Their nasal capsules were inferred to be positioned entirely or partially beneath the rostral plate at the anterior edge of the orbit. In any case, the nasal capsules in *Minicrania* and euantriarchs lie in front of the eyes and far from the pineal opening, similar to the condition in *Brindabellaspis* (King et al., 2018).

By comparison, the nasal capsules in *P. xitunensis* lie beneath the rostral plate between the eyes and just anterior to the pineal opening, similar to *Romundina* and jawless fish. This difference between yunnanolepidoids and advanced antiarchs implies that the nasal capsules underwent a forward migration within antiarchs as the continuation of a tendency inferred from jawless fish to modern gnathostomes (Kuratani and Ahlberg, 2018). The more ‘posterior nose’ in *P. xitunensis* is a primitive condition for antiarchs or placoderms.

Within antiarchs, this forward migration might have a connection with the innovation of the preorbital recess, an apomorphic character for antiarchs (Zhu, 1996; Zhu and Janvier, 1996), and the loss of the preorbital depression (Zhu, 1996). Besides, the proximity between nasal capsules and eyes in *P. xitunensis* implies a short distance between nasal capsules and the telencephalon, or a relatively short olfactory duct. By contrast, the distance between eyes and nasal capsules has dramatically increased at the node uniting *Minicrania*, sinolepids, and euantriarchs (Fig. 4), highlighting the lengthened olfactory ducts.

The paired nasal capsules in *P. xitunensis* at the same level with the eyes, provide concrete evidence to prove the forward migration of nasal capsules in antiarchs. Coupled with the forward migration of nasal capsules from jawless fish to crown jawed vertebrates (Gai et al., 2011; Dupret et al., 2014), the new data imply this forward migration has evolved in parallel in different lineages of jawed stem gnathostomes.

## CONCLUSIONS

Reinvestigation of the headshield of *P. xitunensis* has expanded our knowledge about primitive antiarchs in morphological and anatomical aspects. The suborbital plate of *P. xitunensis* carries a ridge for supporting the palatoquadrate, and contacting the subpremedian ridge on the premedian plate. The sclerotic capsule bears a

large-diameter passage for the eyestalk as in euantriarchs. A relatively small submarginal plate lies above the larger suborbital plate in *P. xitunensis*, in contrast to the condition of euantriarchs. Compared with other yunnanolepids in the post-orbital region of the neurocranium, *P. xitunensis* has two distinguishing features: the development of two pairs of craniospinal processes, and the presence of a postpineal endocranial process. Based on our new data, we revise the previous reconstruction of the sensory canal pattern and the nasal structures. The nasal capsule of *P. xitunensis* beneath the rostral plate at the same level with eyes is primitive for antiarchs or placoderms. By mapping the head conditions onto the new phylogenetic scenario, we infer that the nasal capsules have undergone a forward migration within antiarchs.

## DATA ARCHIVING STATEMENT

Raw X-ray image stacks and reconstruction used in this study are available on the data repository Admorph: <http://www.admorph.org/>. *Parayunnanolepis xitunensis*: IVPP V11679.1, doi: 10.12112/F.180.

## ACKNOWLEDGMENTS

We thank X. C. Guo (IVPP) for suggestions on interpretative drawings, Y. M. Hou (IVPP) for high-resolution CT scanning, W. Gao (IVPP), and L. T. Jia (IVPP) for assistance with photographs. We also thank two reviewers J. Long, M. Brazeau, and the editor C. Burrow for their valuable suggestions to improve the manuscript. The Strategic Priority Research Program of the Chinese Academy of Sciences (grant nos. XDA19050102, XDB26000000), the National Natural Science Foundation of China (grant no. 41530102), and the Key Research Program of Frontier Sciences, CAS (grant no. QYZDJ-SSW-DQC002) supported this research.

## ORCID

Yajing Wang  <http://orcid.org/0000-0002-2230-3526>  
Min Zhu  <http://orcid.org/0000-0002-4786-0898>

## LITERATURE CITED

- Boyle, J., and M. J. Ryan. 2017. New information on *Titanichthys* (Placodermi, Arthrodira) from the Cleveland Shale (Upper Devonian) of Ohio, USA. *Journal of Paleontology* 91:318–336.
- Brazeau, M. D., and M. Friedman. 2015. The origin and early phylogenetic history of jawed vertebrates. *Nature* 520:490–497.
- Cope, E. D. 1885. The position of *Pterichthys* in the system. *Geology and Palaeontology* 19:289–291.
- Dupret, V., S. Sanchez, D. Goujet, and P. E. Ahlberg. 2017. The internal cranial anatomy of *Romundina stellina* Ørvig, 1975 (Vertebrata, Placodermi, Acanthothoraci) and the origin of jawed vertebrates—Anatomical atlas of a primitive gnathostome. *PLoS ONE* 12: e0171241.
- Dupret, V., S. Sanchez, D. Goujet, P. Tafforeau, and P. E. Ahlberg. 2014. A primitive placoderm sheds light on the origin of the jawed vertebrate face. *Nature* 507:500–503.
- Gai, Z.-K., P. C. J. Donoghue, M. Zhu, P. Janvier, and M. Stampanoni. 2011. Fossil jawless fish from China foreshadows early jawed vertebrate anatomy. *Nature* 476:324–327.
- Giles, S., M. Friedman, and M. D. Brazeau. 2015. Osteichthyan-like cranial conditions in an Early Devonian stem gnathostome. *Nature* 520:82–85.
- Goloboff, P. A., and S. A. Catalano. 2016. TNT version 1.5, including a full implementation of phylogenetic morphometrics. *Cladistics* 32:221–238.
- Goujet, D. F. 1984a. Placoderm interrelationships: a new interpretation, with a short review of placoderm classifications. *Proceedings of the Linnean Society of New South Wales* 107:211–243.

- Goujet, D. F. 1984b. Les poissons placodermes du Spitzberg. Arthroires Dolichothoraci de la Formation de Wood Bay (Dévonien inférieur), Volume 15. Editions Centre National Recherche Scientifique, Cahiers de Paléontologie, Paris, 284 pp.
- Goujet, D. F., and G. C. Young. 2004. Placoderm anatomy and phylogeny: new insights; pp. 109–126 in G. Arratia, M. V. H. Wilson, and R. Cloutier (eds.), Recent Advances in the Origin and Early Radiation of Vertebrates. Verlag Dr. Friedrich Pfeil, München.
- Gross, W. 1965. Über die Placodermen-Gattungen *Asterolepis* und *Tiaraspis* aus dem Devon Belgiens und einen fraglichen *Tiaraspis*-rest aus dem Devon Spitzbergens. Institut royal des Sciences naturelles de Belgique, Bulletin 41:1–19.
- Hemmings, S. K. 1978. The Old Red Sandstone antiarchs of Scotland: *Pterichthyodes* and *Microbrachius*. Monographs of the Palaeontographical Society 131:1–64.
- Janvier, P., and J. Pan. 1982. *Hyracaspis bliccki* n.g. n.sp., a new primitive euantiarch (Antiarcha, Placodermi) from the Middle Devonian of northeastern Iran, with a discussion on antiarch phylogeny. Neues Jahrbuch für Geologie und Paläontologie, Abhandlungen 164:364–392.
- Johanson, Z. 1997. New *Remigolepis* (Placodermi; Antiarchi) from Canowindra, New South Wales, Australia. Geological Magazine 134:813–846.
- Johanson, Z., C. Underwood, and M. Richter (eds.). 2019. Evolution and Development of Fishes. Cambridge University Press, Cambridge.
- King, B., G. C. Young, and J. A. Long. 2018. New information on *Brindabellaspis stensioi* Young, 1980, highlights morphological disparity in Early Devonian placoderms. Royal Society Open Science 5:180094.
- Kuratani, S., and P. E. Ahlberg. 2018. Evolution of the vertebrate neurocranium: problems of the premandibular domain and the origin of the trabecula. Zoological Letters 4:1.
- Long, J. A., and L. Werdelin. 1986. A new Late Devonian bothriolepid (Placodermi, Antiarcha) from Victoria, with description of other species from the state. Alcheringa 10:355–399.
- Long, J. A., E. Mark-Kurik, Z. Johanson, M. S. Lee, G. C. Young, M. Zhu, P. E. Ahlberg, M. Newman, R. Jones, J. D. Blauwauw, B. Choo, and K. Trinajstić. 2015. Copulation in antiarch placoderms and the origin of gnathostome internal fertilization. Nature 517:196–199.
- Lukševičs, E. 2001a. The orbito-nasal area of *Asterolepis ornata*, a Middle Devonian placoderm fish. Journal of Vertebrate Paleontology 21:687–692.
- Lukševičs, E. 2001b. Bothriolepid antiarchs (Vertebrata, Placodermi) from the Devonian of the north-western part of the East European Platform. Geodiversitas 23:489–609.
- Lyarskaja, L. 1981. Baltic Devonian Placodermi. Asterolepididae. Zinātnē, Rīga, 152 pp.
- Maddison, W. P., and D. R. Maddison. 2019. Mesquite: a modular system for evolutionary analysis. Version 3.61. Available at [www.mesquiteproject.org](http://www.mesquiteproject.org).
- McCoy, F. 1848. On some new fossil fish from the Carboniferous Period. Annals and Magazine of Natural History 2:1–10, 115–133.
- Miles, R. S. 1968. The Old Red Sandstone antiarchs of Scotland: Family Bothriolepididae. Palaeontographical Society Monographs 122:1–130.
- Miles, R. S. 1971. The Holonematidae (placoderm fishes), a review based on new specimens of *Holonema* from the Upper Devonian of western Australia. Philosophical Transactions of the Royal Society of London, Series B 263:101–234.
- Obruchev, D. V. 1933. Description of four new fish species from the Devonian of Leningrad Province. Materials of the Central Scientific Geological and Prospecting Institute, Palaeontology and Stratigraphy Magazine 1:12–14.
- Ørvig, T. 1975. Description, with special reference to the dermal skeleton, of a new radotiid arthroire from the Gedinnian of Arctic Canada; pp. 41–71 in J. P. Lehman (ed.), Problèmes actuels de Paléontologie-Evolution des Vertébrés. Colloques Internationaux du Centre National de la Recherche Scientifique, Paris.
- Qiao, T., B. King, J. A. Long, P. E. Ahlberg, and M. Zhu. 2016. Early gnathostome phylogeny revisited: multiple method consensus. PLoS ONE 11:e0163157.
- Stensiö, E. A. 1948. On the Placodermi of the Upper Devonian of East Greenland. II. Antiarchi: subfamily Bothriolepinae. With an attempt at a revision of the previously described species of that family. Meddelelser om Grønland 139:1–622.
- Tông-Dzuy, T., and P. Janvier. 1990. Les Vertébrés du Dévonien inférieur du Bac Bo oriental (provinces de Bac Thái et Lang Son, Viêt Nam). Bulletin du Muséum national d'Histoire naturelle, Paris 4e sér., Section C 12:143–223.
- Vaškaninová, V., and P. E. Ahlberg. 2017. Unique diversity of acanthothoracid placoderms (basal jawed vertebrates) in the Early Devonian of the Prague Basin, Czech Republic: A new look at *Radotina* and *Holopetalichthys*. PLoS ONE 12:e0174794.
- Wang, Y. F., C. F. Wei, J. M. Que, W. D. Zhang, C. L. Sun, Y. F. Shu, Y. M. Hou, J. C. Zhang, R. J. Shi, and L. Wei. 2019. Development and applications of paleontological computed tomography. Vertebrata Palasiatica 57:84–92.
- Wang, Y. J., and M. Zhu. 2018. Redescription of *Phymolepis cui Fengshanensis* (Antiarcha: Yunnanolepididae) using high-resolution computed tomography and new insights into anatomical details of the endocranium in antiarchs. PeerJ 6:e4808.
- Young, G. C. 1979. New information on the structure and relationships of *Buchanosteus* (Placodermi: Euarthrodira) from the Early Devonian of New South Wales. Zoological Journal of the Linnean Society 66:309–352.
- Young, G. C. 1980. A new Early Devonian placoderm from New South Wales, Australia, with a discussion of placoderm phylogeny. Palaeontographica Abt. A 167:10–76.
- Young, G. C. 1984. Reconstruction of the jaws and braincase in the Devonian placoderm fish *Bothriolepis*. Palaeontology 27:635–661.
- Young, G. C. 1986. The relationships of placoderm fishes. Zoological Journal of the Linnean Society 88:1–57.
- Young, G. C. 1988. Antiarchs (Placoderm fishes) from the Devonian Aztec Siltstone, Southern Victoria Land, Antarctica. Palaeontographica Abt. A 202:1–125.
- Young, G. C. 1990. New antiarchs (Devonian placoderm fishes) from Queensland, with comments on placoderm phylogeny and biogeography. Memoirs of the Queensland Museum 28:35–50.
- Young, G. C., and G. R. Zhang. 1996. New information on the morphology of yunnanolepid antiarchs (placoderm fishes) from the Early Devonian of South China. Journal of Vertebrate Paleontology 16:623–641.
- Zhang, G. R. 1978. The antiarchs from the Early Devonian of Yunnan. Vertebrata Palasiatica 16:147–186.
- Zhang, G. R., J. Q. Wang, and N. Z. Wang. 2001. The structure of pectoral fin and tail of Yunnanolepidoidei, with a discussion of the pectoral fin of chuchinolepids. Vertebrata Palasiatica 39:1–13.
- Zhang, M. M. 1980. Preliminary note on a Lower Devonian antiarch from Yunnan, China. Vertebrata Palasiatica 18:179–190.
- Zhu, M. 1996. The phylogeny of the Antiarcha (Placodermi, Pisces), with the description of Early Devonian antiarchs from Qujing, Yunnan, China. Bulléin du Muséum national d'Histoire naturelle 18:233–347.
- Zhu, M., and P. Janvier. 1996. A small antiarch, *Minicrania lirouyii* gen. et sp. nov., from the Early Devonian of Qujing, Yunnan (China), with remarks on antiarch phylogeny. Journal of Vertebrate Paleontology 16:1–15.
- Zhu, M., P. E. Ahlberg, Z. H. Pan, Y. A. Zhu, T. Qiao, W. J. Zhao, L. T. Jia, and J. Lu. 2016. A Silurian maxillate placoderm illuminates jaw evolution. Science 354:334–336.
- Zhu, M., X. B. Yu, P. E. Ahlberg, B. Choo, J. Lu, T. Qiao, Q. M. Qu, W. J. Zhao, L. T. Jia, H. Blom, and Y. A. Zhu. 2013. A Silurian placoderm with osteichthyan-like marginal jaw bones. Nature 502:188–193.
- Zhu, Y. A., J. Lu, and M. Zhu. 2019. Reappraisal of the Silurian placoderm *Silurolepis* and insights into the dermal neck joint evolution. Royal Society Open Science 6:191181.

Submitted March 26, 2020; revisions received August 19, 2020; accepted August 27, 2020.

Handling Editor: Carole Burrow.